Axial Observables in $\vec{d}\vec{p}$ Breakup and the Three-Nucleon Force

H. O. Meyer, T. J. Whitaker, R. E. Pollock, B. von Przewoski, T. Rinckel, and J. Doskow
Indiana University Cyclotron Facility, Bloomington, Indiana 47405, USA

J. Kuroś-Żołnierczuk
Nuclear Theory Center, Indiana University, Bloomington, Indiana 47405, USA

P. Thörngren-Engblom
Uppsala University, Uppsala, Sweden

P. V. Pancella
Western Michigan University, Kalamazoo, Michigan 49008, USA

T. Wise
University of Wisconsin, Madison, Wisconsin 53706, USA

B. Lorentz and F. Rathmann
Institut für Kernphysik, Forschungszentrum Jülich, Jülich, Germany
(Received 16 April 2004; published 10 September 2004)

We have measured three axial polarization observables in $\vec{d}\vec{p}$ breakup with a polarized 270 MeV deuteron beam on a polarized proton target. Axial observables are zero by parity conservation in elastic scattering but can be easily observed in the breakup channel at the present energy. Based on a symmetry argument, the sensitivity of these observables to the three-nucleon force might be enhanced. Calculations without three-nucleon force are in fair agreement with our measurement, indicating that the expected sensitivity of axial observables to the three-nucleon force is not confirmed. Including a three-nucleon force in the calculation does not improve the agreement with the data.

DOI: 10.1103/PhysRevLett.93.112502 PACS numbers: 21.30.–x, 21.45.+v, 24.70.+s

The interaction between nucleons, like any exchange force, must on some level include contributions beyond a superposition of pair interactions. Indeed, it is believed that a three-nucleon force (3NF) is required to explain the binding energies of ^{3}H and ^{3}He [1]. On the other hand, an unambiguous manifestation of a 3NF has not yet been established in *pd* or *nd* scattering or breakup observables. An empirical characterization of the 3NF is thus still in the future.

In the past, studies of the 3NF in *pd* or *nd* reactions have often been based on the premise that state-of-the-art Faddeev calculations with modern nucleon-nucleon (*NN*) potentials describe so well how nature *without* a 3NF would present itself that the remaining, small discrepancies with cross section and polarization data must be attributed to the 3NF. In order to select observables that are most sensitive to the 3NF one would have to rely on calculations with and without a theoretical three-nucleon potential. However, the currently available theoretical 3NFs do not lead to a better agreement with the data, which include cross sections and many polarization observables at energies up to the pion threshold (see, e.g., [2]). It would thus be preferable to have a more fundamental criterion to identify 3NF-sensitive observables.

Knutson [3] has pointed out that so-called "axial" observables may have an enhanced sensitivity to the 3NF. By definition, these polarization observables are antisymmetric under space inversion. If parity is conserved, such observables vanish when the momenta of the beam and of all reaction products lie in a common plane, as is the case for elastic scattering, but not, in general, for the breakup reaction. Knutson's argument is based on quantum numbers and small energies and states that axial observables are likely to be sensitive to a certain kind of spin operator that can occur in three-nucleon potentials, but not in the interaction between nucleon pairs. Thus, axial observables are linked, in principle, to the 3NF, and may exhibit enhanced 3NF sensitivity.

Whether the 3N spin operators contribute significantly to axial observables must be established by experiment. An attempt to do this is described in Ref. [4], which reports the measurement of the longitudinal proton analyzing power A_z in $\vec{p}d$ breakup at a proton bombarding energy of $T_p = 9$ MeV. The reported analyzing powers are zero within the experimental uncertainty (typically ± 0.01), and consistent with a corresponding Faddeev calculation.

Here, we present the measurement of three of the five axial observables that can be observed in the $\vec{d}\vec{p}$ breakup using a polarized deuteron beam on a polarized proton target. The beam energy is $T_d = 270$ MeV, which is equivalent to $T_p = 135$ MeV proton bombarding energy.

In the following we briefly describe the experiment; more details can be found in Ref. [5]. The deuteron beam from a polarized ion source was accumulated and accelerated to 90 MeV in an injector synchrotron and transferred to the Cooler storage ring, where it was electron cooled and accelerated to the final energy. After taking data for 110 s, the remaining beam was discarded and the cycle was repeated. For a new cycle, the beam polarization was changed to the next of five polarization states, including (i) positive vector ($Q_\zeta \sim +0.8$), (ii) negative vector ($Q_\zeta \sim -0.6$), (iii) pure tensor ($Q_{\zeta\zeta} \sim +0.8$), (iv) pure negative tensor polarization ($Q_{\zeta\zeta} \sim -1.6$), and (v) unpolarized beam. States (i) and (ii) contained a tensor polarization admixture ($Q_{\zeta\zeta} \sim +0.7$). The quoted values of the vector and tensor polarizations, Q_ζ and $Q_{\zeta\zeta}$, are with respect to the spin alignment axis and represent approximate average values. The relevant polarization moments follow from the orientation of the spin alignment axis, which throughout the experiment was vertical.

The target was produced by a source of polarized H atoms [6]; the atomic beam was aimed through a fill tube into a 25 cm long, 12 mm diameter, thin-walled (25 μm) aluminum storage cell through which the stored beam passed. The thickness of the extended target was a few times 10^{13} atoms/cm^2. The cell position could be adjusted remotely with respect to the stored beam to minimize reactions in the cell wall. Magnetic fields in the region of the target cell were used to produce one of six polarization directions, i.e., vertical, sideways, or longitudinal, each with both directions. The average target polarization was $P \sim 0.6$.

The azimuthally symmetric detector covered a forward cone of about a 45° half angle and was capable of measuring the direction and energy of charged particles. In the beam direction, it contained a thin scintillator (F), two pairs of wire chambers, a 15 cm thick scintillator array (K) divided into quadrants, and a 10 cm thick scintillator array (E) divided into octants. All detectors had a hole in the center to accommodate the stored beam. All particles of interest were stopped in K and E. Protons were distinguished from deuterons, based on stopped energy and energy loss in F. All events with a response in at least two segments of K were written to disk. Breakup events (two protons in coincidence) were selected by conditions on the reconstructed tracks, matching of the tracks with the scintillator segments, particle identification, and a match of the reconstructed mass of the unobserved particle with the actual neutron mass.

Concurrently with the breakup data, elastic scattering events, with a coplanar proton and deuteron in coincidence, were also registered, covering the polar angle range $76° < \theta_{\rm cm} < 140°$. These events are crucial since they provide a sample of particles of known energy, needed to deduce an absolute energy calibration of the K and E detectors, and because they also provide the beam and target polarizations by comparison to previously measured pd scattering polarization observables [2,7–9].

To describe the beam and target polarization moments and the kinematics of an event, we define a fixed Cartesian frame with the z axis in the beam direction, the y axis upwards, and the x axis to the left, completing a right-handed frame. Polar angles θ are measured from the z axis, and azimuths ϕ from the x axis, clockwise if viewed in the beam direction. Since for breakup events, the energy and direction of both protons in the final state are known, the experiment is kinematically complete; i.e., all five kinematic variables are determined. To further process these events, we deduce the center-of-mass momentum vector $\vec{q}$ of the neutron and $\vec{p}$, the relative momentum of the two protons. Since the two detected particles are identical, we arbitrarily define $\vec{p}$ such that it points into the forward direction ($p_z > 0$). The five independent kinematic variables are then θ_p, θ_q, ϕ_p, ϕ_q, and $|\vec{p}|$.

Axial polarization observables are invariant under rotations around the z axis and can depend only on the difference $\Delta\phi \equiv \phi_p - \phi_q$ between the two azimuths. This reduces the number of kinematic variables to four. Retaining only terms with rotational symmetry around the z axis, and only terms that can be measured with a *vertical* deuteron spin alignment axis, the differential cross section σ for a $\vec{d}\vec{p}$ reaction with polarized collision partners (see, e.g., [10]) becomes

$$\begin{aligned}\sigma = \sigma_0[1 &+ \tfrac{1}{2}q_{zz}A_{zz} + \tfrac{3}{4}(q_x p_x + q_y p_y)(C_{x,x} + C_{y,y}) \\ &+ p_z A_z + \tfrac{3}{4}(q_y p_x - q_x p_y)(C_{y,x} - C_{x,y}) \\ &+ \tfrac{1}{2}q_{zz}p_z C_{zz,z}].\end{aligned} \tag{1}$$

In this expression, the p_m ($m = x, y, z$) are the components of the proton polarization (magnitude P), the q_m are the components of the deuteron vector polarization (magnitude Q_ζ), and q_{zz} is the only tensor moment that plays a role. For a vertical spin alignment axis, $q_{zz} = -\frac{1}{2}Q_{\zeta\zeta}$. The observables (here in a Cartesian basis) include the proton analyzing power A_z, the tensor analyzing power A_{zz}, two combinations of vector correlation coefficients, and the tensor correlation coefficient $C_{zz,z}$; all of these are a function of θ_p, θ_q, $|\vec{p}|$, and $\Delta\phi$. The terms on the first line of Eq. (1) are related to "normal" observables, unconstrained by parity conservation, while the remainder contains axial observables, which change sign under a reflection on the x-z plane, i.e., $O(\Delta\phi) = O(-\Delta\phi)$ [3]. The two remaining axial observables A_z^d and $C_{xz,x} - C_{yz,y}$

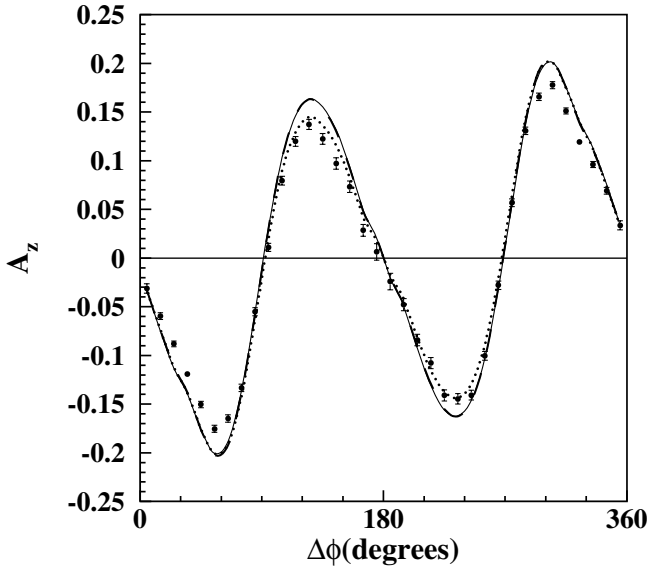

FIG. 1. Longitudinal proton analyzing power as a function of $\Delta\phi$. The solid and dashed curves are based on the CD-Bonn and the AV18 *NN* interaction, respectively. When the TM′ three-nucleon potential is combined with the CD-Bonn interaction, the dotted curve results.

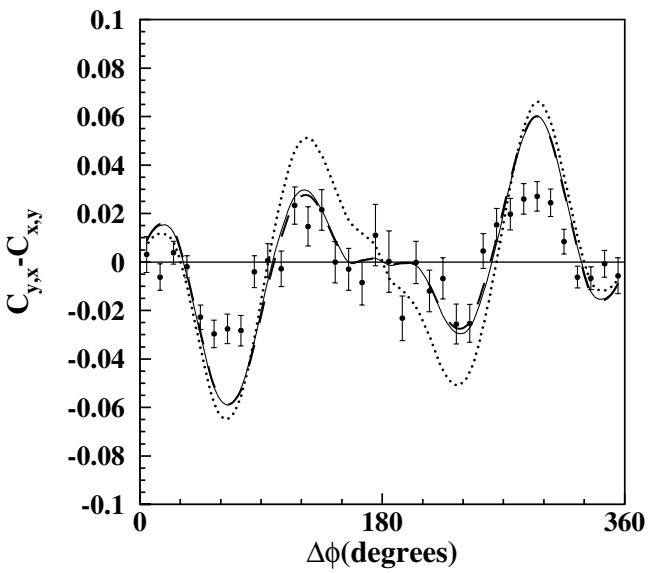

FIG. 2. Vector correlation coefficient $C_{y,x} - C_{x,y}$ as a function of $\Delta\phi$. The curves are explained in the caption for Fig. 1.

cannot be measured with vertical deuteron spin alignment.

By combining the yields measured with the appropriate combinations of the five beam and six target polarization states, individual terms in Eq. (1) are singled out. The data are evaluated as a function of $\Delta\phi$. The other three kinematic variables are ignored; thus their full range within the detector acceptance is included.

Figure 1 shows the longitudinal proton analyzing power A_z as a function of $\Delta\phi$. This observable involves longitudinal target polarization of both signs, combined with an average over the five beam states, and thus includes one-third of the breakup events collected in all spin directions (about 5×10^7). The axial vector correlation coefficient ($C_{y,x} - C_{x,y}$) versus $\Delta\phi$, which uses data with a vector-polarized beam, combined with sideways target polarization is shown in Fig. 2. Finally, Fig. 3 shows the tensor correlation coefficient $C_{zz,z}$, which is derived from the beam states with tensor polarization, combined with longitudinal target polarization. As expected, all three axial observables presented here cross zero at $\Delta\phi = 0$ and $\Delta\phi = \pi$, i.e., for coplanar final-state configurations. The error bars shown represent statistical uncertainties. An overall normalization uncertainty arises from the determination of the beam and target polarization (1.5% for A_z and 4% for the other two observables).

When comparing an experimental result with theory, breakup reactions have the inherent problem that the calculation has to be averaged over all kinematic variables that are not explicitly used in quoting a result. This average has to be weighted by the cross section and the probability that the detector registers an event at a given point ξ in phase space. To do this is often difficult: for the present experiment, for instance, the acceptance angle of the detector depends on the location of the event along the extended target, there is a lower limit for the energy of protons that reach the trigger detector, the joints between detector segments may locally reduce the efficiency, and so on.

In order to take instrumental constraints into account correctly, we have developed a new method [11], which is

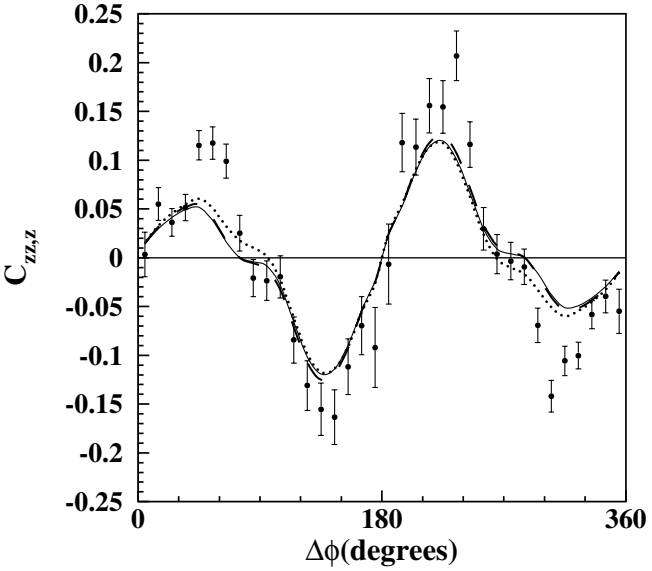

FIG. 3. Tensor correlation coefficient $C_{zz,z}$ as a function of $\Delta\phi$. The curves are explained in the caption for Fig. 1.

applicable for any kinematically complete experiment. This method is based on the notion that the local density of measured events at some phase space point ξ represents the proper weight that should be used when averaging the theoretical expectation. It can then be shown that the theoretical expectation, properly averaged over a given phase space region η, which could, for instance, consist of a $\Delta\phi$ bin with unconstrained remaining variables, is simply given by

$$\langle O^{\mathrm{th}}(\eta)\rangle = \frac{1}{N(\eta)} \sum_{i=1}^{N(\eta)} O^{\mathrm{th}}(\xi_i), \tag{2}$$

where ξ_i represents the four kinematic parameters of the ith event and $N(\eta)$ is the number of events in region η. The uncertainty due to the stochastic sampling, and corrections due to polarization effects that are not averaged out by summing over all events, are discussed in Ref. [11] but are not important in this context. To evaluate Eq. (2), one needs to calculate the observable O^{th} for each event. In order to do this efficiently, we use a uniform four-dimensional grid that spans all of phase space. At each grid point the observable value is calculated from the Faddeev amplitudes. The value for $O^{\mathrm{th}}(\xi_i)$ is then obtained from this table of numbers by interpolation. The solid line in Figs. 1–3 shows the expectation from a Faddeev calculation [12] based on the CD-Bonn nucleon-nucleon potential [13]. In order to explore the dependence on the choice of the NN interaction, the dashed line represents a calculation with the AV18 potential [14]. As can be seen, the two calculations are nearly identical. The effect of including a theoretical 3NF (in this case, the TM′ potential [15]) is illustrated by the dotted line.

For A_z the collected statistics is sufficient to explore the dependence of this observable on any of the kinematic variables over which we have averaged so far. This dependence turns out to be generally flat. Moreover, the effect of including the 3NF in the calculation is still small and shows no significant variation as a function of these variables (for more detail, see Ref. [16]). Thus, we can dismiss the worry that interesting information may be lost by averaging over phase space.

From our results and the calculations presented in Figs. 1–3, we conclude the following:

(i) We have observed nonzero values for the longitudinal analyzing power in pd breakup, as well as for two additional observables that are also forbidden in reactions with a two-body final state. This is the first experimental verification that axial observables in pd breakup can differ from zero and, in fact, be quite large. This may indicate that at the present energy axial observables are dominated by 2N contributions, which in turn would dilute the sensitivity to the 3NF, discussed by Knutson [3].

(ii) If axial observables were indeed especially sensitive to the 3NF, we would expect that calculations without a 3NF would differ significantly from the data. Instead, we find that these calculations already provide a fairly good description of the measurements. The remaining discrepancies are quite similar to those found in polarization observables in elastic scattering at the same energy. Thus, we conclude that the sensitivity of the axial observables reported here to the 3NF is not enhanced as we had hoped.

(iii) The difference between the measured A_z and the calculation without a 3NF is reduced by the inclusion of the TM′ 3NF at some angles but not at others. For the other two observables the TM′ 3NF does nothing or moves the calculation in the wrong direction. Based on the present data, we conclude that either the difference between the data and the calculation without a 3NF is not due to the 3NF, or the TM′ potential is not a valid description of the 3NF.

The authors wish to thank Terry Sloan, Gary East, and the members of the Operations Group, Brian Allen, Pete Goodwin, Glen Hendershot, Mark Luxnat, Tom Meaden, and John Ostler for their hard work at odd hours. This work has been carried out under NFS Grant No. PHY-0100348, DOE Grant No. FG0288ER40438, and Grant No. Dnr 629-2001-3868 from the Swedish Research Council.

[1] A. Nogga, H. Kamada, and W. Glöckle, Phys. Rev. Lett. **85**, 944 (2000).
[2] B. v. Przewoski *et al.*, Phys. Rev. C (to be published).
[3] L. D. Knutson, Phys. Rev. Lett. **73**, 3062 (1994).
[4] E. A. George *et al.*, Phys. Rev. C **54**, 1523 (1996).
[5] T. Rinckel *et al.*, Nucl. Instrum. Methods Phys. Res., Sect. A **439**, 117 (2000).
[6] T. Wise, A. Roberts, and W. Haeberli, Nucl. Instrum. Methods Phys. Res., Sect. A **336**, 410 (1993).
[7] H. Sakai *et al.*, Phys. Rev. Lett. **84**, 5288 (2000).
[8] N. Sakamoto *et al.*, Phys. Lett. B **367**, 60 (1996).
[9] K. Ermisch *et al.*, Phys. Rev. Lett. **86**, 5862 (2001).
[10] G. G. Ohlsen, Rep. Prog. Phys. **35**, 717 (1972).
[11] J. Kuroś-Żołnierczuk *et al.*, Few-Body Syst. **34**, 259 (2004).
[12] W. Glöckle *et al.*, Phys. Rep. **274**, 107 (1996).
[13] R. Machleidt, Phys. Rev. C **63**, 024001 (2001).
[14] R. B. Wiringa, V. G. Stoks, and R. Schiavilla, Phys. Rev. C **51**, 38 (1995).
[15] S. A. Coon and W. Glöckle, Phys. Rev. C **23**, 1790 (1981).
[16] T. J. Whitaker, Ph.D. thesis, Indiana University, 2004.